AIMS Mathematics, 9(6): 16146–16167.
DOI: 10.3934/math.2024781
Received: 01 February 2024
Revised: 15 April 2024
Accepted: 17 April 2024
Published: 08 May 2024

http://www.aimspress.com/journal/Math

Research article

The Riccati-Bernoulli sub-optimal differential equation method for analyzing the fractional Dullin-Gottwald-Holm equation and modeling nonlinear waves in fluid mediums

Humaira Yasmin[1,2,*], Haifa A. Alyousef[3], Sadia Asad[4], Imran Khan[5], R. T. Matoog[6] and S. A. El-Tantawy[7,8,*]

[1] Department of Basic Sciences, General Administration of Preparatory Year, King Faisal University, P.O. Box 400, Al Ahsa 31982, Saudi Arabia
[2] Department of Mathematics and Statistics, College of Science, King Faisal University, P.O. Box 400, Al Ahsa 31982, Saudi Arabia
[3] Department of Physics, College of Science, Princess Nourah bint Abdulrahman University, P.O. Box 84428, Riyadh 11671, Saudi Arabia
[4] Department of Architecture and Interior Design, College of Engineering, Majmaah University, Al-Majmaah 11952, Saudi Arabia
[5] Department of Mathematics and Statistic, Bacha Khan University, Charsadda, Pakistan
[6] Mathematics Department, Faculty of Sciences, Umm Al-Qura University, Makkah, Saudi Arabia
[7] Department of Physics, Faculty of Science, Port Said University, Port Said 42521, Egypt
[8] Research Center for Physics (RCP), Department of Physics, Faculty of Science and Arts, Al-Mikhwah, Al-Baha University, Al-Baha 1988, Saudi Arabia

* **Correspondence:** Email: hhassain@kfu.edu.sa, tantawy@sci.psu.edu.eg.

Abstract: The present study investigates the fractional Dullin-Gottwald-Holm equation by using the Riccati-Bernoulli sub-optimal differential equation method with the Bäcklund transformation. By employing a well-established criterion, the present study reveals novel cusp soliton solutions that resemble peakons and offers valuable insights into their dynamic behaviors and mysterious phenomena. The solution family encompasses various analytical solutions, such as peakons, periodic, and kink-wave solutions. Furthermore, the impact of both the time- and space-fractional parameters on all derived solutions' profiles is examined. This investigation's significance lies in its contribution to understanding intricate dynamics inside physical systems, offering valuable insights into various domains like fluid mechanics and nonlinear phenomena across different physical models. The computational technique's straightforward, effective, and concise nature is demonstrated through introduction of some graphical representations in two- and three-dimensional plots generated by adjusting the related parameters. The findings underscore the versatility of this methodology and

demonstrate its applicability as a tool to solve more complicated nonlinear problems as well as its ability to explain many mysterious phenomena.

Keywords: fractional Dullin-Gottwald-Holm equation; Bäcklund transformation; Riccati-Bernoulli sub-optimal differential equation method; traveling wave solutions

1. Introduction

In recent times, academics have been increasingly interested in finding analytical solutions to some nonlinear partial differential equations that describe and model various physical and engineering problems, including fluid dynamics, plasma astrophysics, ocean engineering, and nonlinear optics [1–6]. These equations function as mathematical representations that encapsulate the complexities of intricate physical occurrences. These models have broad applications in various nonlinear scientific fields such as fluid mechanics, biology, chemistry, physics, plasmas, and optical fibers. Their applicability highlights their relevance in explaining and forecasting the behavior of complex systems across various scientific fields. To better understand the dynamics of these real-world components, methods for solving fractional nonlinear partial differential equations (PDEs) must be investigated [7–11]. This exploration is necessary to study and understand the complex behaviors inherent in the systems above. Solutions to nonlinear fractional PDEs (FPDEs) are of academic interest because of the increased detail and generality they provide, as they outperform traditional solutions in terms of descriptive power. In addition to improving our understanding and predictive capabilities in these vital areas of nonlinear physics, this study has implications for a wide range of real-world applications because it clarifies nonlinear aspects. Researchers in the field of nonlinear physics have significantly contributed to our knowledge of complex processes in various other scientific fields [12–16].

The investigation of analytical solutions for FPDEs is intrinsically tricky, and it has led to the creation of many mathematical strategies to address this complex issue. Because analytical solutions can offer a comprehensive understanding of fundamental physical processes and show the precise behavior of the modeled system beyond what can be achieved by using numerical approaches, analysts are particularly drawn to them. Consequently, pursuing analytical solutions for FPDEs is recognized as a crucial and continuously developing field of study [17–19]. Various mathematical techniques have been employed in scholarly literature to solve different types of FPDEs efficiently and analytically [20–24]. This demonstrates the extensive scope of research in this field. Numerous strategies have been employed, showing the diversity of approaches that researchers in this discipline have chosen [25–27]. Among the approaches under consideration, several techniques [28–36] have emerged as noteworthy contributors. Every approach has unique benefits, broadening the toolkit of techniques that can be used to solve FPDEs and improving our understanding of these complex mathematical models [37, 38].

Furthermore, integrated into the structure of the suggested methodology, the Riccati-Bernoulli sub-optimal differential equation (ODE) method [39–41] is a powerful tool. It is well known for its adept management of complex algebraic calculations and ability to derive solutions for a wide range of phenomena that occur in applications such as biology, chemistry, physics, fluid mechanics, and

optical fibers. This methodology has significant potential for use in several scientific and engineering fields. Its application in the fields of biological systems, industrial operations, and environmental flows can facilitate a deep understanding of the complexities of fluid behavior, thereby improving optimization and forecasting methods. The FPDEs are transformed into an algebraic system by using the Bäcklund transformation and the Riccati-Bernoulli equation, simplifying the extraction of important information from the intricate dynamics present in these systems. This method greatly enhances our understanding of the underlying physical mechanisms. The methodology is particularly noteworthy because it guarantees the derivation of finite solutions, thereby validating the precision and effectiveness of solutions for the equations under examination. A critical feature of this approach is its potential to produce a wide range of single-wave solutions, increasing its adaptability and usefulness.

Moreover, the current study was designed to utilize an analytical approach to clarify the complex dynamics of the Dullin-Gottwald-Holm (DGH) equation [42]. This study also looks at how linear dispersion parameters change the shape of traveling waves that are connected to the DGH equation and the isospectral features of soliton solutions. It should be mentioned here that the DGH equation was derived from asymptotic expansions applied directly to the Hamiltonian driving Euler equations, and it was first developed as a model for unidirectional shallow water waves over a flat bottom

$$F_t + \lambda F_x + 3FF_x - \mu^2 \left(F_{xxt} + FF_{xxx} + 2F_xF_{xx}\right) + \chi F_{xxx} = 0. \tag{1.1}$$

The DGH equation is linked to two distinct soliton equations that govern water waves and can be integrated independently. The DGH equation (1.1) specifically can be reduced to the well-known Korteweg-de Vries (KdV) equation for ($\mu = 0$) and ($\chi \neq 0$): $F_t + \lambda F_x + 3FF_x + \chi F_{xxx} = 0$. In contrast, the DGH equation (1.1) can be reduced to the Camassa-Holm (CH) equation for ($\mu = 1$) and ($\chi = 0$): $F_t + \lambda F_x + 3FF_x - (F_{xxt} + FF_{xxx} + 2F_xF_{xx}) = 0$. This two-way connection shows how the DGH equation can be used to describe different wave events and how it can be used to combine the dynamics given by the KdV and CH equations in certain parameter situations. Numerous studies have been carried out to clarify the DGH equation of integer order. Dullin et al. [43] revealed another integrable instance in the DGH formula. A thorough treatment of the Cauchy problem related to the DGH equation was conducted in a different study [44]. Tang and Yang [45] extended the peakon equations by introducing an integral constant and using the dynamical systems bifurcation approach. Chen et al. [46] used the Darboux transformation technique to produce numerous soliton solutions. Zhang et al. [47] focused on peakons and periodic cusp wave solutions for a generalized CH equation by using the bifurcation theory of planar dynamical systems. Liu [48] explored questions about the creation of singularities and the existence of global solutions. Under the condition that $\mu^2 < 0$, Dullin et al. [49] showed that there are three different kinds of limited waves for the DGH equation. These different studies contribute to the development of a more thorough knowledge of the complex dynamics of the DGH equation for various parameter values. Regarding tasks that involve obtaining a precise description of complex nonlinear systems in a variety of scientific fields, such as fluid dynamics and oceanography, nonlinear dynamics and soliton theory, mathematical physics, numerical simulations, computational mathematics, and engineering, the fractional DGH equation is considered to be an essential tool to describe systems that display complex structures and subtle nonlinearities. The fractional DGH equation has the following mathematical expression:

$$(D_t^{\alpha}(F)) + \lambda D_x^{\beta}(F) + 3FD_x^{\beta}(F)$$

$$-\mu^2\left(D_t^{\alpha}(D_x^{2\beta}(F)) + FD_x^{3\beta}(F) + 2D_x^{\beta}(F)D_x^{2\beta}(F)\right) + \chi D_x^{3\beta}(F) = 0, \tag{1.2}$$

with $0 < \alpha, \beta, \leq 1$, where α and β indicate the time- and space-fractional parameters, respectively.

The height of the free surface over a flat bottom is represented by the function $F(x,t)$, and the coefficient (χ) indicates the linear dispersive parameter and the linear wave speed for undisturbed water at rest at spatial infinity is represented by $(\lambda = 2\omega = \sqrt{gh})$. Here, (g) indicates the gravitational constant, (h) denotes the mean fluid depth, and (ω) represents the essential shallow water speed for undisturbed water at rest at spatial infinity. The Greek symbol (μ^2) represents square length scales. The operator representing the order α derivatives adheres to the definition provided in [50]:

$$D_{\theta}^{\alpha}q(\theta) = \lim_{m\to 0}\frac{q(m(\theta)^{1-\alpha} - q(\theta))}{m}, 0 < \alpha \leq 1. \tag{1.3}$$

This inquiry utilizes the following characteristics of this derivative:

$$\begin{cases} D_{\theta}^{\alpha}\left(j_1\eta(\theta) \pm j_2 m(\theta)\right) = j_1 D_{\theta}^{\alpha}(\eta(\theta)) \pm j_2 D_{\theta}^{\alpha}(m(\theta)), \\ D_{\theta}^{\alpha}\chi\left[\xi^{\tau}(\theta)\right] = \chi'_{\xi}(\xi(\theta))D_{\theta}^{\alpha}\xi(\theta). \end{cases} \tag{1.4}$$

Hence, the primary motivation and goal of this investigation is to use the Riccati-Bernoulli sub-ODE method with the help of the Bäcklund transformation in order to analyze and solve the fractional DGH equation, as this method has not been used before to analyze this equation. We study how linear dispersion factors affect the shape of traveling waves in the DGH equation and look into the isospectral properties of soliton solutions. Through these analyses, our research advances knowledge by revealing new perspectives on the fundamental mechanisms underlying complicated occurrences, thus positioning itself as a ground-breaking undertaking in the scientific debate.

A meticulous and systematic approach has been adopted to structure the manuscript. A detailed exposition of the methods employed in Section 2 serves to elucidate the intricacy of the approach. Section 3 meticulously outlines the process of problem execution by using the described methodology. Section 4 offers a comprehensive discussion and synthesis of the results. Finally, Section 5 provides a succinct summary of the study's definitive findings and their broad implications.

2. Methodology

The FPDE described herein warrants consideration:

$$P_1\left(f, D_t^{\alpha}(f), D_{\zeta_1}^{\beta}(f), D_{\zeta_2}^{2\beta}(f), fD_{\zeta_1}^{\beta}(f), \ldots\right) = 0, \quad 0 < \alpha, \beta, \leq 1. \tag{2.1}$$

The polynomial P_1 is a function of $f(\zeta_1, \zeta_2, \zeta_3, ..., t)$. This polynomial includes the fractional order derivatives as well as the nonlinear terms. The fundamental phases of this approach are then comprehensively addressed. The subsequent wave transformations are our recommendations for investigating potential solutions for Eq (1.2):

$$F(x,t) = e^{i\psi}f(\psi), \tag{2.2}$$

with

$$\psi(x,t) = \left(\frac{x^{\beta}}{\beta}\right) - \kappa\left(\frac{t^{\alpha}}{\alpha}\right). \tag{2.3}$$

The function $\psi \equiv \psi(x,t)$ represents the transformation of propagating waves. The non-zero constant (κ) gives the traveling wave dynamics distinctive properties. Equation (1.2) undergoes a change that results in the construction of a nonlinear optimal differential equation; as a result, a modified mathematical expression is assumed. This modification represents an intrinsic change in the equation's structure, going from its original form to a nonlinear form. This change brings new dynamics and behaviors; hence, a better mathematical model is required

$$P_2\left(f, f'(\psi), f''(\psi), ff'(\psi), \ldots\right) = 0. \tag{2.4}$$

Consider the formal solution for Eq (2.4)

$$f(\psi) = \sum_{i=-N}^{N} b_i \varphi(\psi)^i. \tag{2.5}$$

Under the restriction that both $b_N \neq 0$ and $b_{-N} \neq 0$ simultaneously, the b_i constants must be determined. Concurrently, the function is generated via the following Bäcklund transformation

$$\varphi(\psi) = \frac{-\tau B + A\phi(\psi)}{A + B\phi(\psi)}. \tag{2.6}$$

With the requirement that $B \neq 0$, let (τ), (A), and (B) be constants. Furthermore, suppose that $\phi(\psi)$ is a function that has the following definition:

$$\frac{d\phi}{d\psi} = \tau + \phi(\psi)^2. \tag{2.7}$$

It is commonly acknowledged that the following formulas indicate the solutions to Eq (2.7) [51]:

$$(i) \quad \text{If} \quad \tau < 0, \quad \text{then} \quad \phi(\psi) = -\sqrt{-\tau}\tanh(\sqrt{-\tau}\psi), \quad \text{or} \quad \phi(\psi) = -\sqrt{-\tau}\coth(\sqrt{-\tau}\psi). \tag{2.8}$$

$$(ii) \quad \text{If} \quad \tau > 0, \quad \text{then} \quad \phi(\psi) = \sqrt{\tau}\tan(\sqrt{\tau}\psi), \quad \text{or} \quad \phi(\psi) = -\sqrt{\tau}\cot(\sqrt{\tau}\psi). \tag{2.9}$$

$$(iii) \quad \text{If} \quad \tau = 0, \quad \text{then} \quad \phi(\psi) = \frac{-1}{\psi}. \tag{2.10}$$

Under the framework of Eq (2.5), the positive integer (N) can be determined by using homogeneous balancing principles, which entail finding an equilibrium between the highest-order derivatives and the highest nonlinearity in Eq (2.4). Here, the $f(\psi)$ degree can be expressed more precisely as $D[f(\psi)] = N$. Therefore, this enables us to perform the following computation of the degree of linked expressions:

$$D\left[\frac{d^k f}{d\psi^k}\right] = N + k \;\&\; D\left[f^J \frac{d^k f}{d\psi^k}\right]^s = NJ + s(k+N). \tag{2.11}$$

Algebraic equations are established by combining Eq (2.4) with Eqs (2.5) and (2.7), grouping terms with the same powers of $f(\psi)$, and then equating them to zero. Applying Maple software to deduce the pertinent values for various parameters will result in an efficient resolution of this system. Thus, this makes it easier to compute the soliton wave-propagating solutions to Eq (1.2) with accuracy by performing computational analysis.

3. Execution of the problem

By employing the methodology outlined in Section 2, we systematically resolve the fractional DGH equation (1.2), focusing on obtaining solutions that include a single wave. Equation (2.3), which characterizes the wave transformation, is employed to streamline our investigation within the framework of the fractional DGH equation. Subsequently, we give the resulting equation i.e, an inferred nonlinear ODE, which describes the nonlinear dynamics after this transformation. This new formula is a concise formulation of the original FPDE and marks a significant step forward in comprehending the underlying dynamics in the fractional DGH framework

$$-\kappa f' + \lambda f' + 3\left(f' f\right) - \mu^2\left[-\kappa f''' + f''' f + 2 f' f''\right] + \chi f''' = 0, \tag{3.1}$$

which is equivalent to

$$f'\left(\lambda - \kappa\right) + 3 f f' + \mu^2 \kappa f''' - \mu^2 f f''' - 2\mu^2 f' f'' + \chi f''' = 0. \tag{3.2}$$

Integrating Eq (3.2) once over ψ, with zero constantss of integration, we obtain

$$f\left(\lambda - \kappa\right) + \frac{3}{2} f^2 + \mu^2 \kappa f'' - \mu^2 f f'' + \frac{\mu^2}{2}\left(f'\right)^2 - \mu^2\left(f'\right)^2 + \chi f'' = 0. \tag{3.3}$$

Re-arranging Eq (3.3), we get

$$\left(\mu^2 f - \kappa\mu^2 - \chi\right) f'' + \frac{1}{2}\mu^2\left(f'\right)^2 - \left(\lambda - \kappa\right) f - \frac{3}{2} f^2 = 0. \tag{3.4}$$

Finding the point of homogeneous equilibrium ($N = 2$) entails striking a harmonious balance between the highest nonlinearity and the highest-order derivatives in the given equation: $2N = N + 2 \longmapsto N = 2$. Now incorporate the substitution from Eq (2.5) along with Eqs (2.6) and (2.7) into Eq (3.4). We systematically gather coefficients for $\phi^i(\psi)$, resulting in an algebraic system of equations with a zero value. With the help of Maple's computing capacity, we can solve this system of algebraic equations and obtain the following solutions. This approach guarantees an organized and effective extraction of solutions, providing insightful information about the interactions between variables within the given mathematical framework

$$b_0 = -\tfrac{1}{2}\tfrac{\lambda\mu^2+\chi}{\mu^2}, b_1 = \sqrt{2}\sqrt{-\lambda\left(\lambda\mu^2+\chi\right)}, \tau = \tfrac{1}{2\mu^2}, \kappa = -\tfrac{1}{4}\tfrac{\lambda\mu^2+3\chi}{\mu^2}, \tag{3.5}$$

The other parameters are as follows: $b_{-1} = b_{-2} = b_2 = 0$ and $B = B$. Accordingly, the value of ψ given in Eq (2.3) is given by

$$\psi = \frac{x^\beta}{\beta} + \frac{1}{4}\frac{\left(\lambda\mu^2 + 3\chi\right)t^\alpha}{\mu^2\alpha}. \tag{3.6}$$

Solution Set 1: For $\tau < 0$, the following solutions for Eq (1.2) are obtained

$$F_1(x,t) = -\frac{1}{2}\frac{\left(\lambda\mu^2+\chi\right)e^{i\psi}}{\mu^2} + \sqrt{2}\sqrt{-\lambda\left(\lambda\mu^2+\chi\right)}e^{i\psi}\frac{\left[-\frac{1}{2}\frac{B}{\mu^2} - \frac{1}{2}A\sqrt{-\frac{2}{\mu^2}}\tanh\left(\frac{1}{2}\sqrt{-\frac{2}{\mu^2}}\psi\right)\right]}{\left[A - \frac{1}{2}B\sqrt{-\frac{2}{\mu^2}}\tanh\left(\frac{1}{2}\sqrt{-2\mu^{-2}}\psi\right)\right]}, \tag{3.7}$$

or

$$F_2(x,t) = -\frac{1}{2}\frac{\left(\lambda\mu^2+\chi\right)e^{i\psi}}{\mu^2} + \sqrt{2}\sqrt{-\lambda\left(\lambda\mu^2+\chi\right)}e^{i\psi}\frac{\left[-\frac{1}{2}\frac{B}{\mu^2} - \frac{1}{2}A\sqrt{-\frac{2}{\mu^2}}\coth\left(\frac{1}{2}\sqrt{-\frac{2}{\mu^2}}\psi\right)\right]}{\left[A - \frac{1}{2}B\sqrt{-\frac{2}{\mu^2}}\coth\left(\frac{1}{2}\sqrt{-\frac{2}{\mu^2}}\psi\right)\right]}. \tag{3.8}$$

Solution Set 2: For $\tau > 0$, the following solutions for Eq (1.2) are obtained

$$F_3(x,t) = -\frac{1}{2}\frac{\left(\lambda\mu^2+\chi\right)e^{i\psi}}{\mu^2} + \sqrt{2}\sqrt{-\lambda\left(\lambda\mu^2+\chi\right)}e^{i\psi}\frac{\left[-\frac{1}{2}\frac{B}{\mu^2} + \frac{1}{2}A\sqrt{\frac{2}{\mu^2}}\tan\left(\frac{1}{2}\sqrt{\frac{2}{\mu^2}}\psi\right)\right]}{\left[A + \frac{1}{2}B\sqrt{\frac{2}{\mu^2}}\tan\left(\frac{1}{2}\sqrt{\frac{2}{\mu^2}}\psi\right)\right]} \tag{3.9}$$

or

$$F_4(x,t) = -\frac{1}{2}\frac{\left(\lambda\mu^2+\chi\right)e^{i\psi}}{\mu^2} + \sqrt{2}\sqrt{-\lambda\left(\lambda\mu^2+\chi\right)}e^{i\psi}\frac{\left[-\frac{1}{2}\frac{B}{\mu^2} - \frac{1}{2}A\sqrt{\frac{2}{\mu^2}}\cot\left(\frac{1}{2}\sqrt{\frac{2}{\mu^2}}\psi\right)\right]}{\left[A - \frac{1}{2}B\sqrt{\frac{2}{\mu^2}}\cot\left(\frac{1}{2}\sqrt{\frac{2}{\mu^2}}\psi\right)\right]}. \tag{3.10}$$

Solution Set 3: For $\tau = 0$, the following solutions for Eq (1.2) are obtained

$$F_5(x,t) = -\frac{1}{2}\frac{\left(\lambda\mu^2+\chi\right)e^{i\psi}}{\mu^2} + \sqrt{2}\sqrt{-\lambda\left(\lambda\mu^2+\chi\right)}e^{i\psi}\frac{\left(-\frac{1}{2}\frac{B}{\mu^2} - \frac{A}{\psi}\right)}{\left(A - \frac{B}{\psi}\right)}. \tag{3.11}$$

4. Results and discussion

This study offers a useful instrument for researchers interested in exploring the intriguing applications of the fractional DGH equation, as it is a mathematical model that characterizes the propagation of waves in shallow water. The Riccati-Bernoulli sub-ODE method was used in this study to look at wave structure solutions for the nonlinear fractional DGH problem. By exploring their underlying nonlinear physics, this research offers valuable insights into the behavior of complex systems and illuminates phenomena that have remained incompletely understood thus far. Figures 1–10 visually represent some derived solutions, utilizing 3D and 2D graphics to emphasize the parameter choices for the fractional DGH model. Furthermore, utilizing 2D plots facilitates the modeling and depiction of analytical physical phenomena.

We analyzed all of the derived solutions graphically, as shown in Figures 1–10, by using some random values for the associated parameters and coefficients of the equation. The absolute value of the solution given by Eq (3.7) was examined as elucidated in Figures 1 and 2, which was evaluated against the space- and time-fractional parameters β and α, respectively. As shown in Figure 1, increasing the space-fractional parameter turns the shock wave into a quasi-peakon wave. The impact of the time-fractional parameter on the characteristics of the quasi-peakon wave is illustrated in Figure 2. Furthermore, an investigation was conducted to examine the impact of space- and time fractional parameters β and α on the profile of the solution given by Eq (3.8), as depicted in Figures 3 and 4, respectively. Based on the data presented in Figure 3, it can be observed that for $\alpha = 1$, when

the space-fractional parameter β is altered, the solution's form remains consistent with the shock wave's shape. However, as β increases, the shock wave amplitude decreases. Figure 4 further illustrates the impact of the time-fractional parameter α on the visual representation of the solution given by Eq (3.8), which exhibits characteristics akin to a peakon waveform. The solutions given by Eqs(3.9) and (3.10) for the case that $\tau > 0$ are also examined, as depicted in Figures 5–8. Figures 5 and 6 display the shock-like solution given by Eq (3.9) against both the space- and time-fractional parameters β and α, respectively. Additionally, we analyzed the influence of both the space- and time-fractional parameters β and α on the characteristics of the solution given by Eq (3.10), as depicted in Figures 7 and 8, correspondingly. Ultimately, we conducted a graphical analysis of the quasi-peakon wave solution given by Eq (3.11) and examined the impact of both the space- and time-fractional parameters β and α on its behavior, as depicted in Figures 9 and 10, respectively.

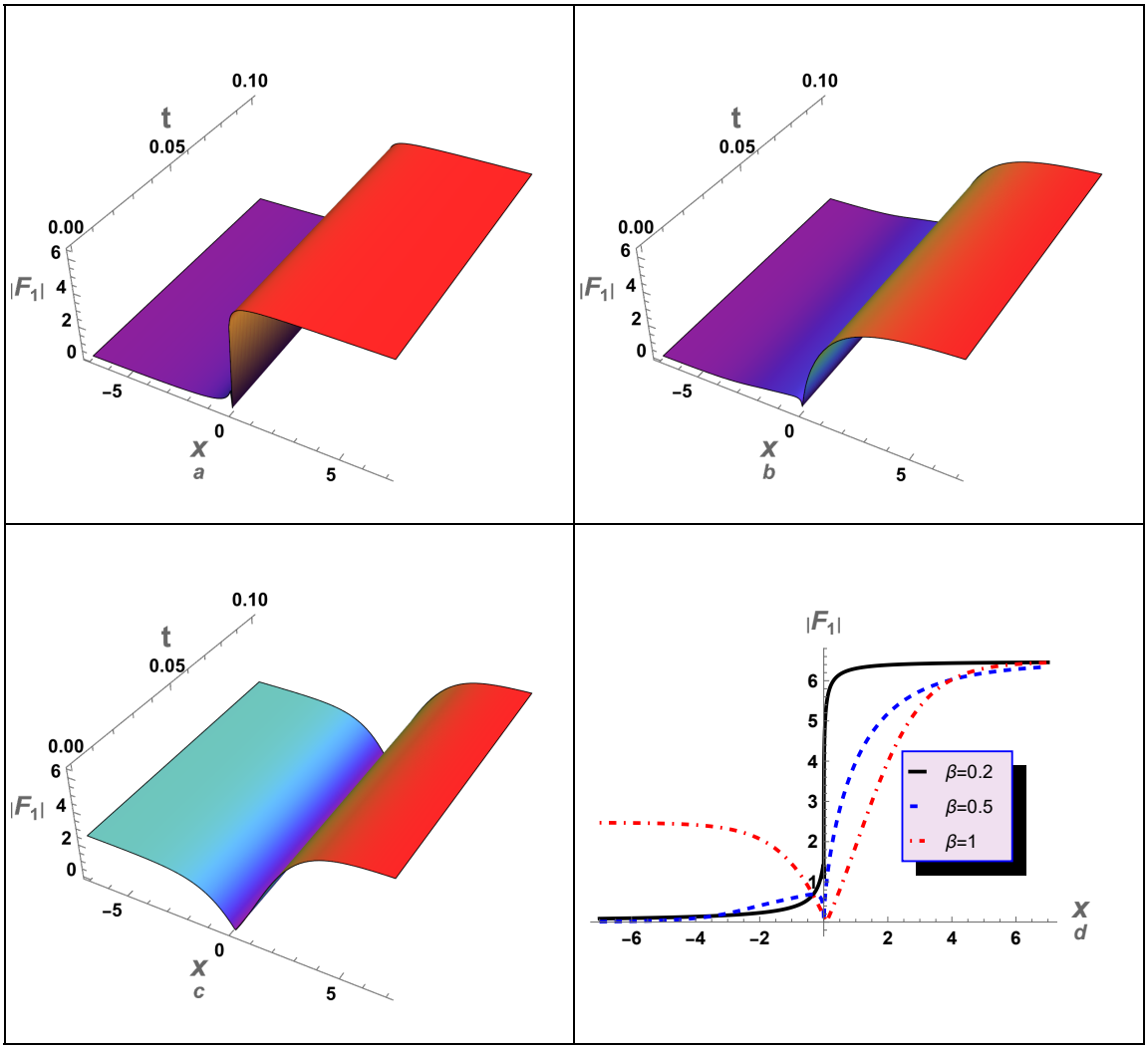

Figure 1. The solution $|F_1(x,t)|$ is plotted against the space-fractional parameter β: (a) 3D graphic for the solution given by Eq (3.7) at $\beta = 0.2$, (b) 3D graphic for the solution given by Eq (3.7) at $\beta = 0.5$, (c) 3D graphic for the solution given by Eq (3.7) at $\beta = 1$, (d) 2D graphic for the solution given by Eq (3.7) at different values of β. Here, $\alpha = 1$, $\lambda = 5$, $\mu = \sqrt{-2}, \chi = 2$, $A = 1$, and $B = 1$.

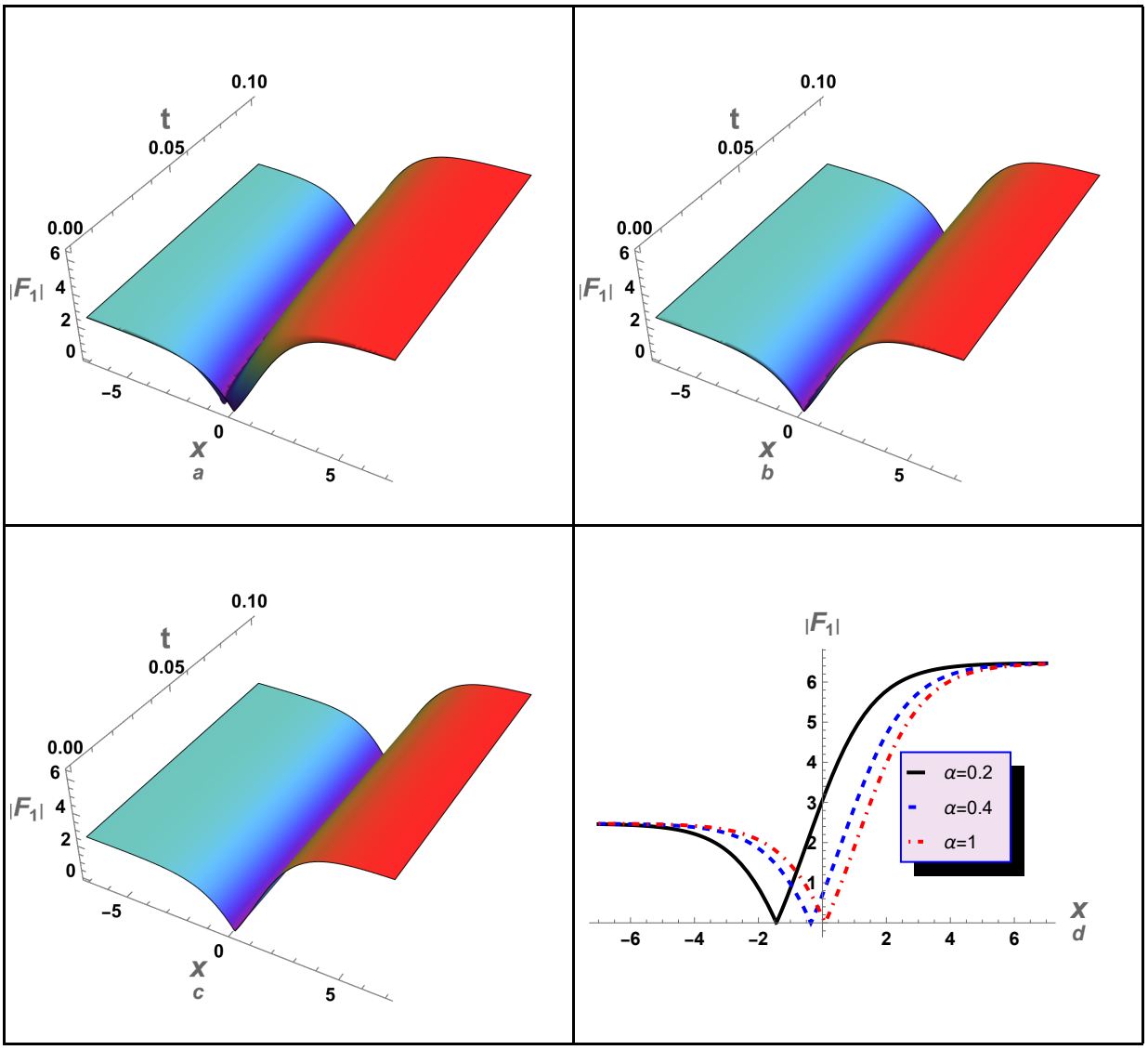

Figure 2. The solution $|F_1(x,t)|$ is plotted against the time-fractional parameter α: (a) 3D graphic for the solution given by Eq (3.7) at $\alpha = 0.2$, (b) 3D graphic for the solution given by Eq (3.7) at $\alpha = 0.4$, (c) 3D graphic for the solution given by Eq (3.7) at $\alpha = 1$, (d) 2D graphic for the solution given by Eq (3.7) at different values of α. Here, $\beta = 1$, $\lambda = 5$, $\mu = \sqrt{-2}$, $\chi = 2$, $A = 1$, and $B = 1$.

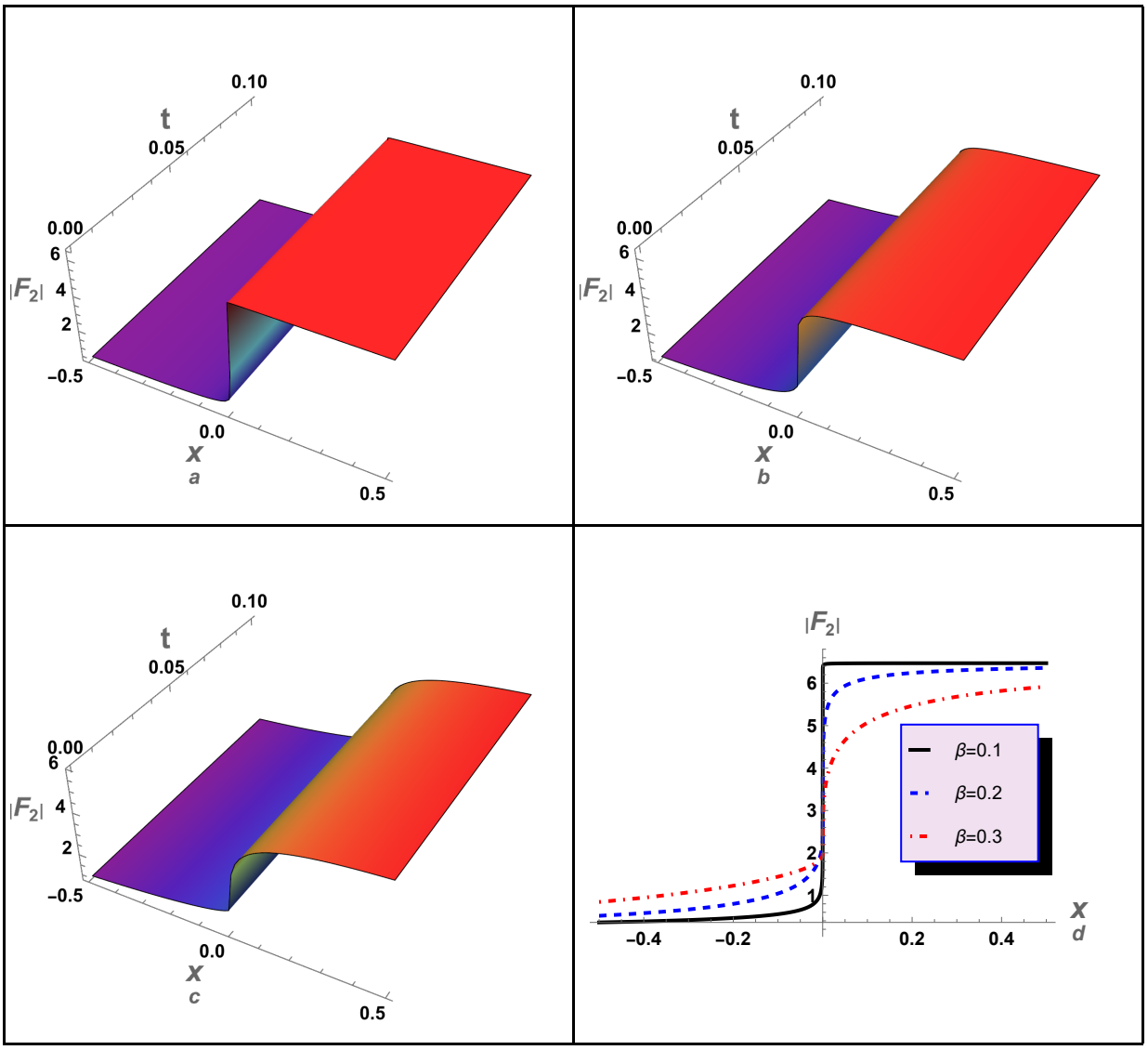

Figure 3. The solution $|F_2(x,t)|$ is plotted against the space-fractional parameter β: (a) 3D graphic for the solution given by Eq (3.8) at $\beta = 0.1$, (b) 3D graphic for the solution given by Eq (3.8) at $\beta = 0.2$, (c) 3D graphic for the solution given by Eq (3.8) at $\beta = 0.3$, (d) 2D graphic for the solution given by Eq (3.8) at different values of β. Here, $\alpha = 1$, $\lambda = 5$, $\mu = \sqrt{-2}$, $\chi = 2$, $A = 0.1$, and $B = 10$.

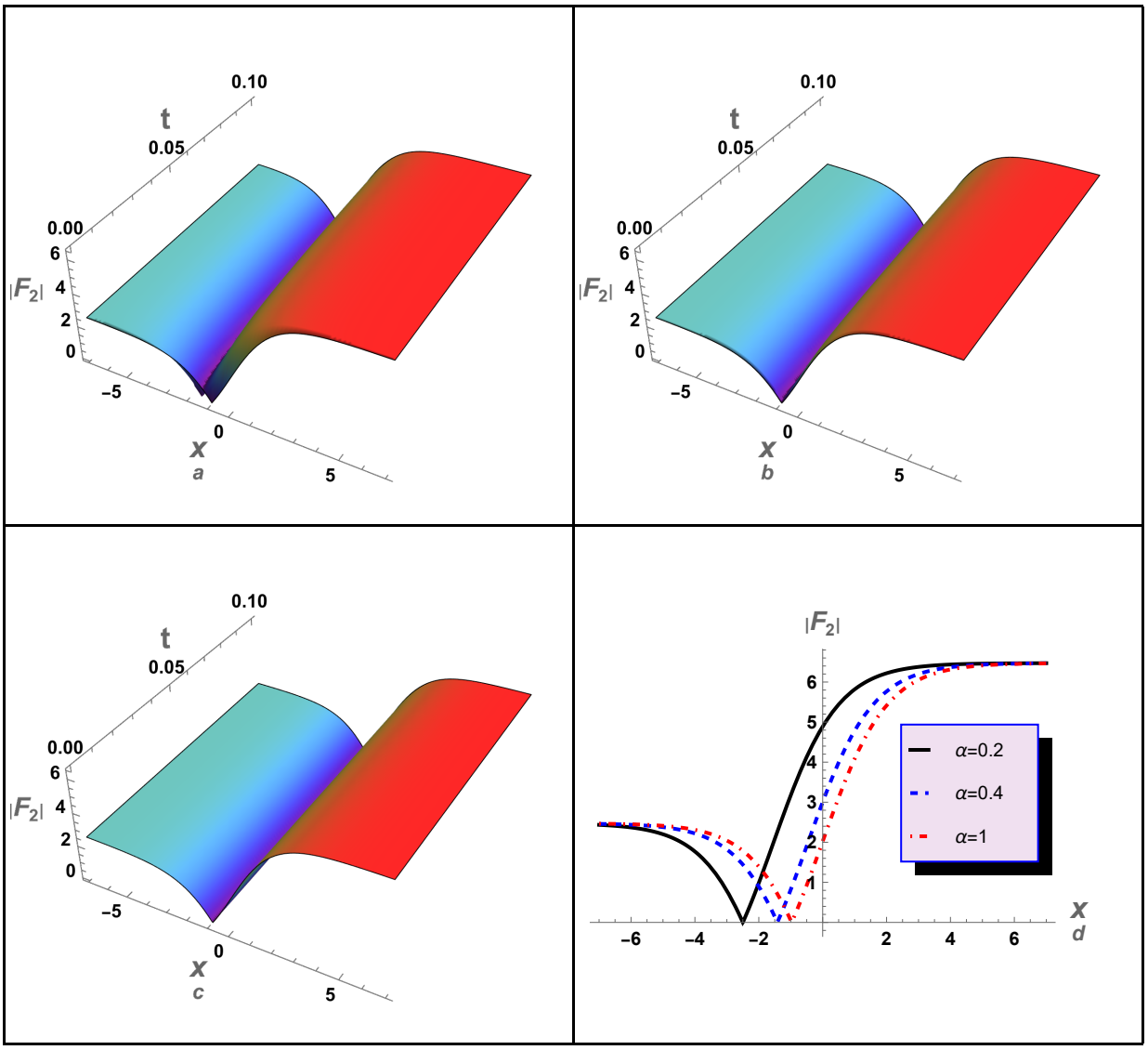

Figure 4. The solution $|F_2(x,t)|$ is plotted against the time-fractional parameter α: (a) 3D graphic for the solution given by Eq (3.8) at $\alpha = 0.2$, (b) 3D graphic for the solution given by Eq (3.8) at $\alpha = 0.4$, (c) 3D graphic for the solution given by Eq (3.8) at $\alpha = 1$, (d) 2D graphic for the solution given by Eq (3.8) at different values of α. Here, $\beta = 1$, $\lambda = 5$, $\mu = \sqrt{-2}$, $\chi = 2$, $A = 0.1$, and $B = 10$.

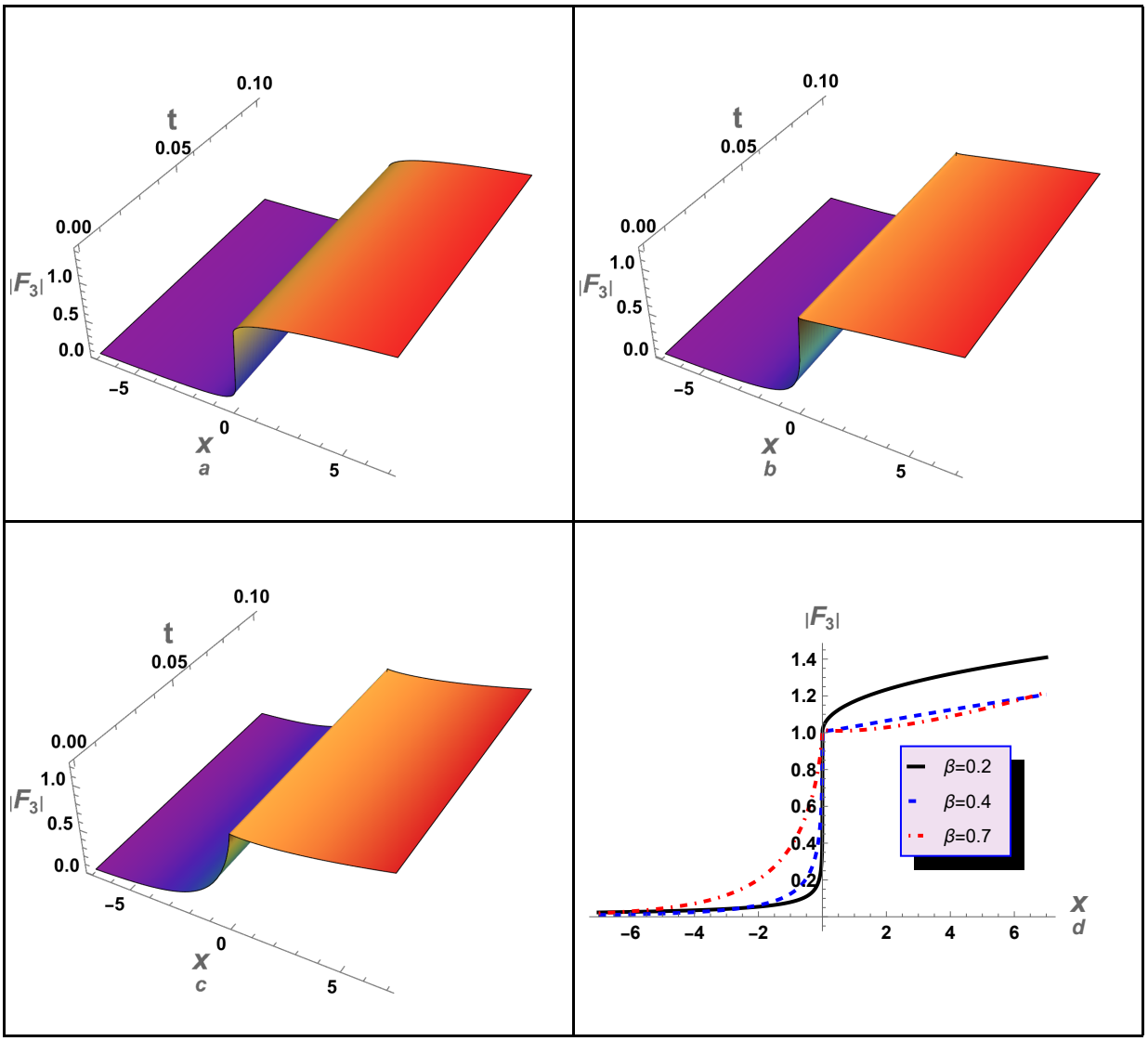

Figure 5. The solution $|F_3(x,t)|$ is plotted against the space-fractional parameter β: (a) 3D graphic for the solution given by Eq (3.9) at $\beta = 0.2$, (b) 3D graphic for the solution given by Eq (3.9) at $\beta = 0.4$, (c) 3D graphic for the solution given by Eq (3.9) at $\beta = 0.7$, (d) 2D graphic for the solution given by Eq (3.9) at different values of β. Here, $\alpha = 1$, $\lambda = 2$, $\mu = 10$, $\chi = 2$, $A = 1$, and $B = 1$.

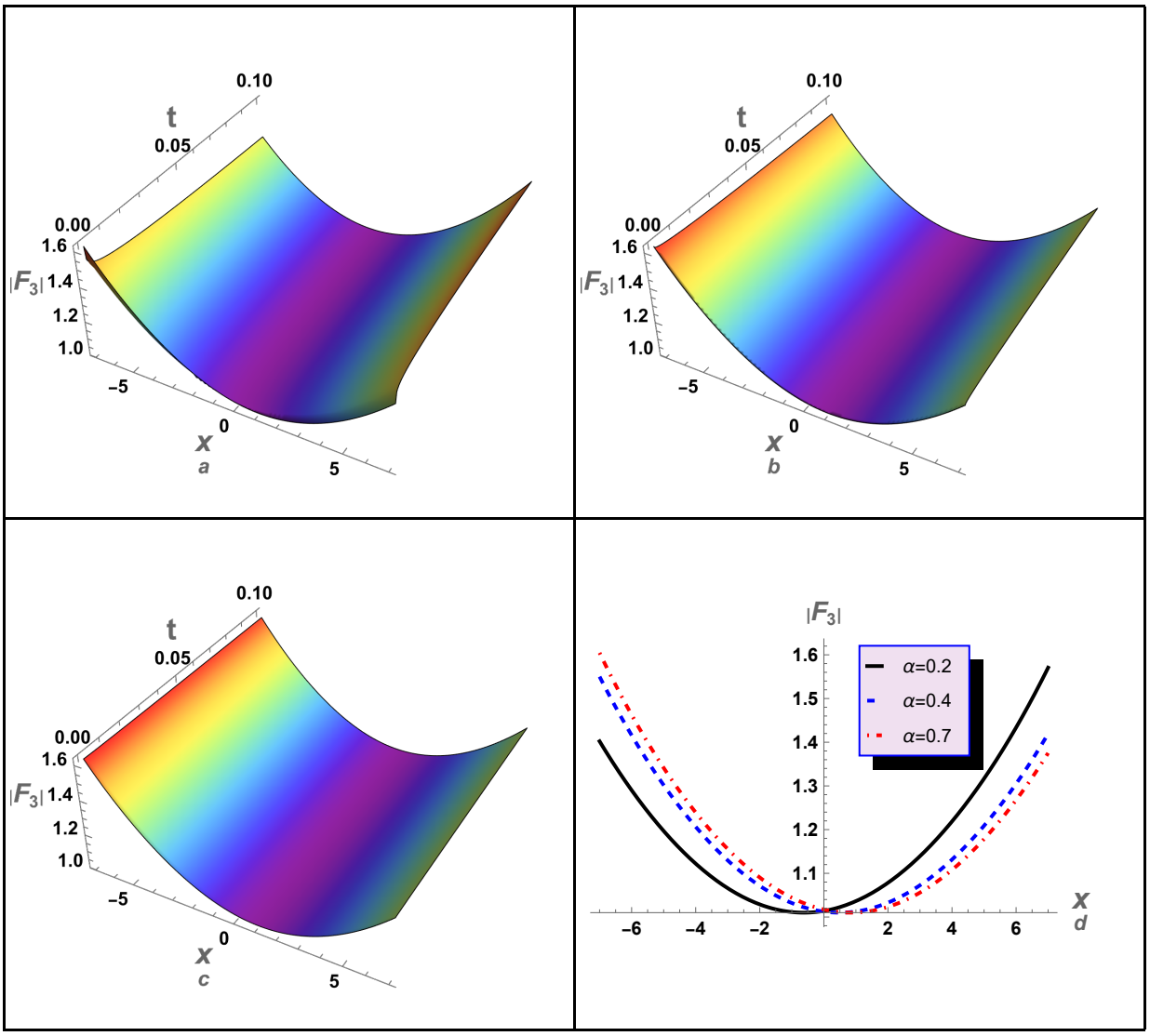

Figure 6. The solution $|F_3(x,t)|$ is plotted against the time-fractional parameter α: (a) 3D graphic for the solution given by Eq (3.9) at $\alpha = 0.2$, (b) 3D graphic for the solution given by Eq (3.9) at $\alpha = 0.4$, (c) 3D graphic for the solution given by Eq (3.9) at $\alpha = 0.7$, (d) 2D graphic for the solution given by Eq (3.9) at different values of α. Here, $\beta = 1$, $\lambda = 2$, $\mu = 10$, $\chi = 2$, $A = 1$, and $B = 1$.

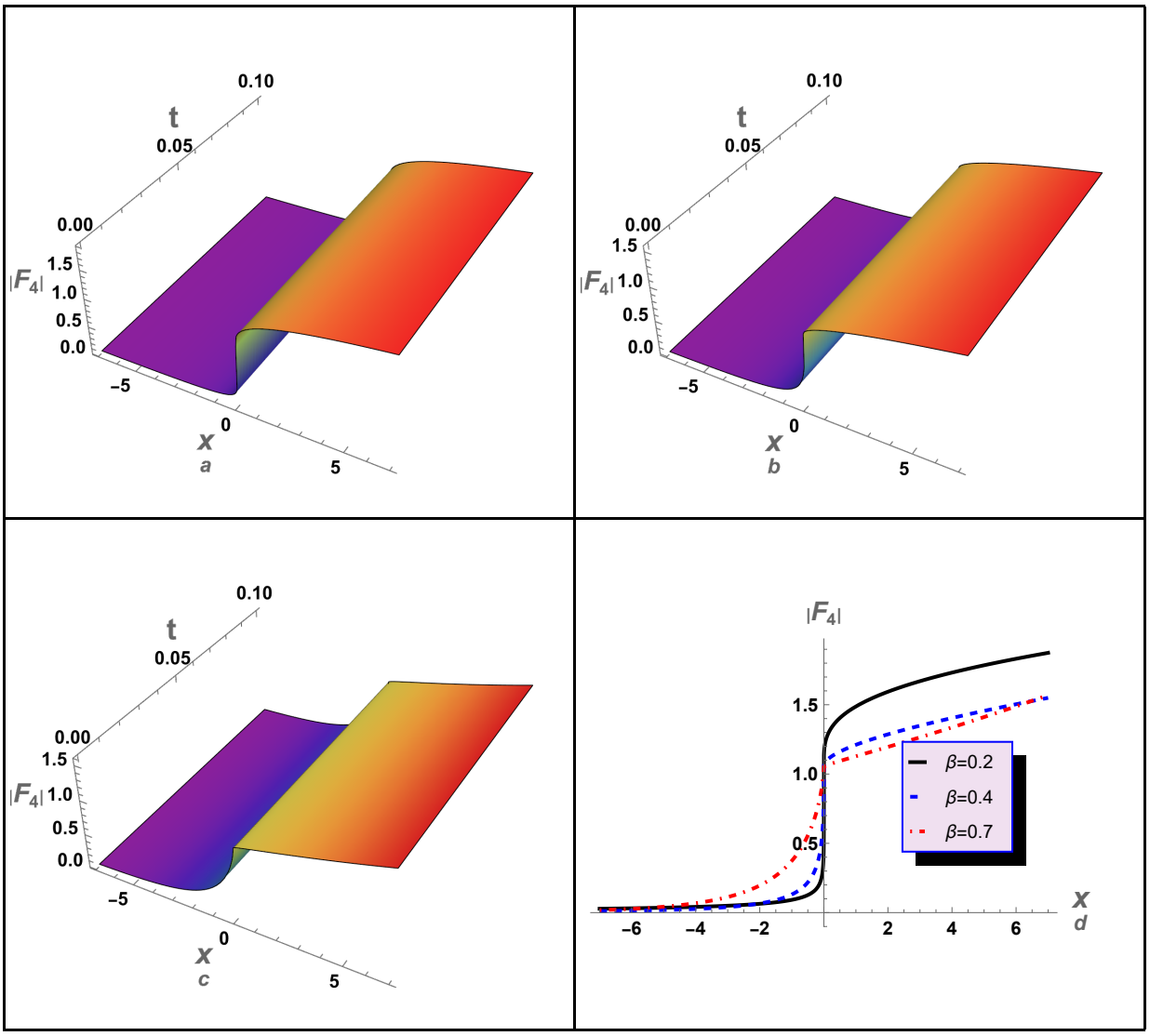

Figure 7. The solution $|F_4(x,t)|$ is plotted against the space-fractional parameter β: (a) 3D graphic for the solution given by Eq (3.10) at $\beta = 0.2$, (b) 3D graphic for the solution given by Eq (3.10) at $\beta = 0.4$, (c) 3D graphic for the solution given by Eq (3.10) at $\beta = 0.7$, (d) 2D graphic for the solution given by Eq (3.10) at different values of β. Here, $\alpha = 1$, $\lambda = 2$, $\mu = 10$, $\chi = 2$, $A = 0.1$, and $B = 10$.

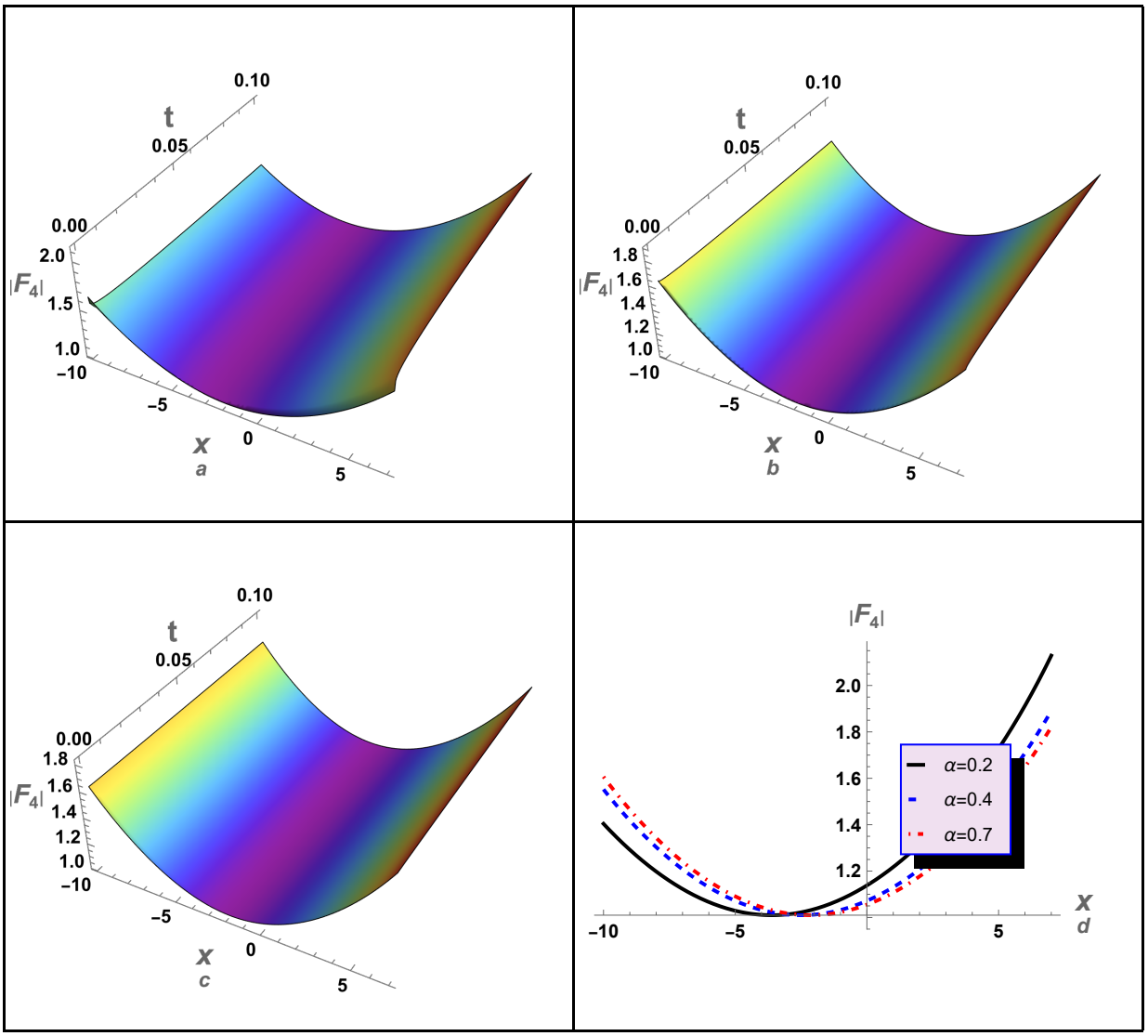

Figure 8. The solution $|F_4(x,t)|$ is plotted against the time-fractional parameter α: (a) 3D graphic for the solution given by Eq (3.10) at $\alpha = 0.2$, (b) 3D graphic for the solution given by Eq (3.10) at $\alpha = 0.4$, (c) 3D graphic for the solution given by Eq (3.10) at $\alpha = 0.7$, (d) 2D graphic for the solution given by Eq (3.10) at different values of α. Here, $\beta = 1$, $\lambda = 2$, $\mu = 10$, $\chi = 2$, $A = 0.1$, and $B = 10$.

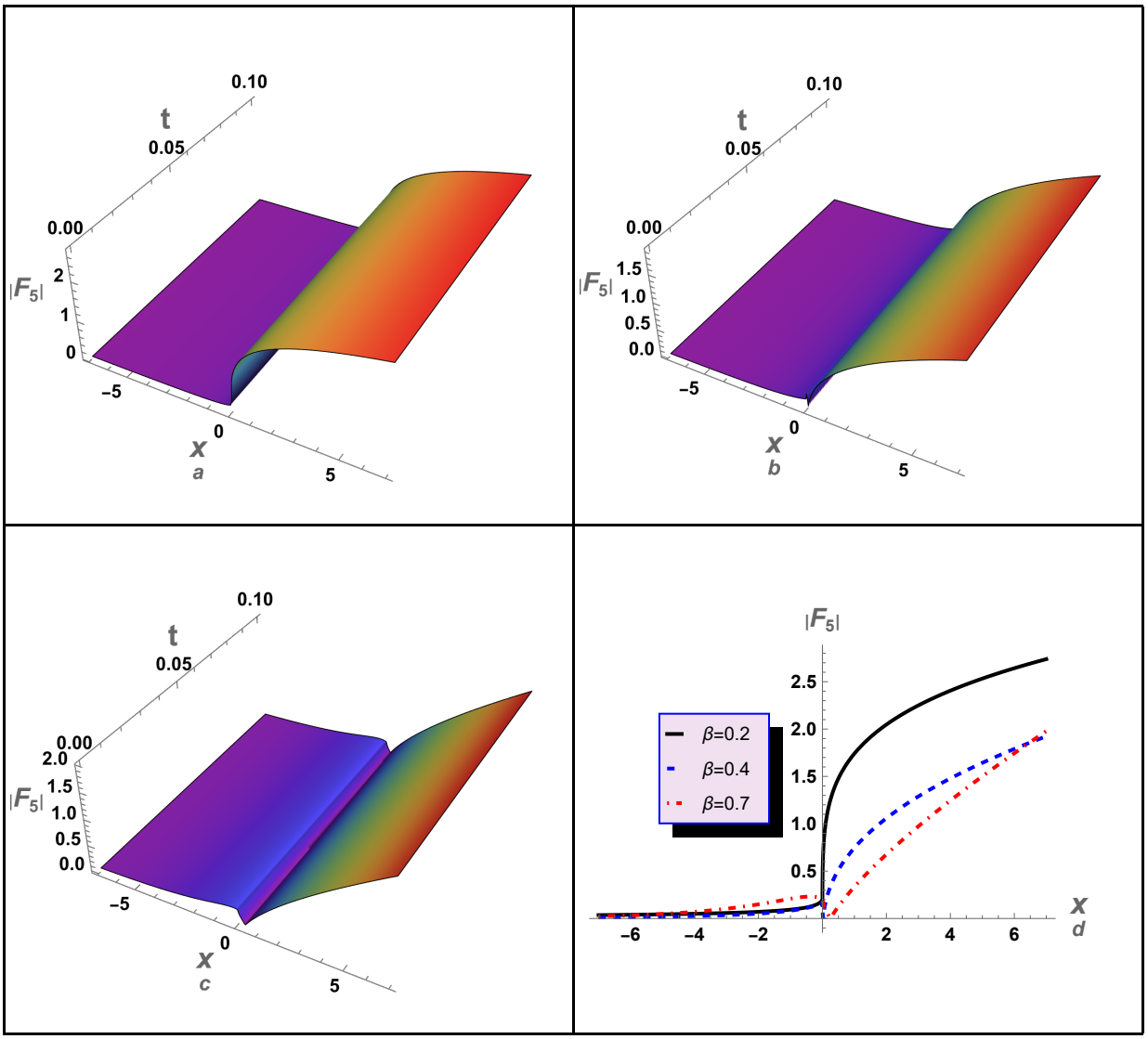

Figure 9. The solution $|F_5(x,t)|$ is plotted against the space-fractional parameter β: (a) 3D graphic for the solution given by Eq (3.11) at $\beta = 0.2$, (b) 3D graphic for the solution given by Eq (3.11) at $\beta = 0.4$, (c) 3D graphic for the solution given by Eq (3.11) at $\beta = 0.7$, (d) 2D graphic for the solution given by Eq (3.11) at different values of β. Here, $\alpha = 1$, $\lambda = -2$, $\mu = -2$, $\chi = 10$, $A = 0.1$, and $B = 10$.

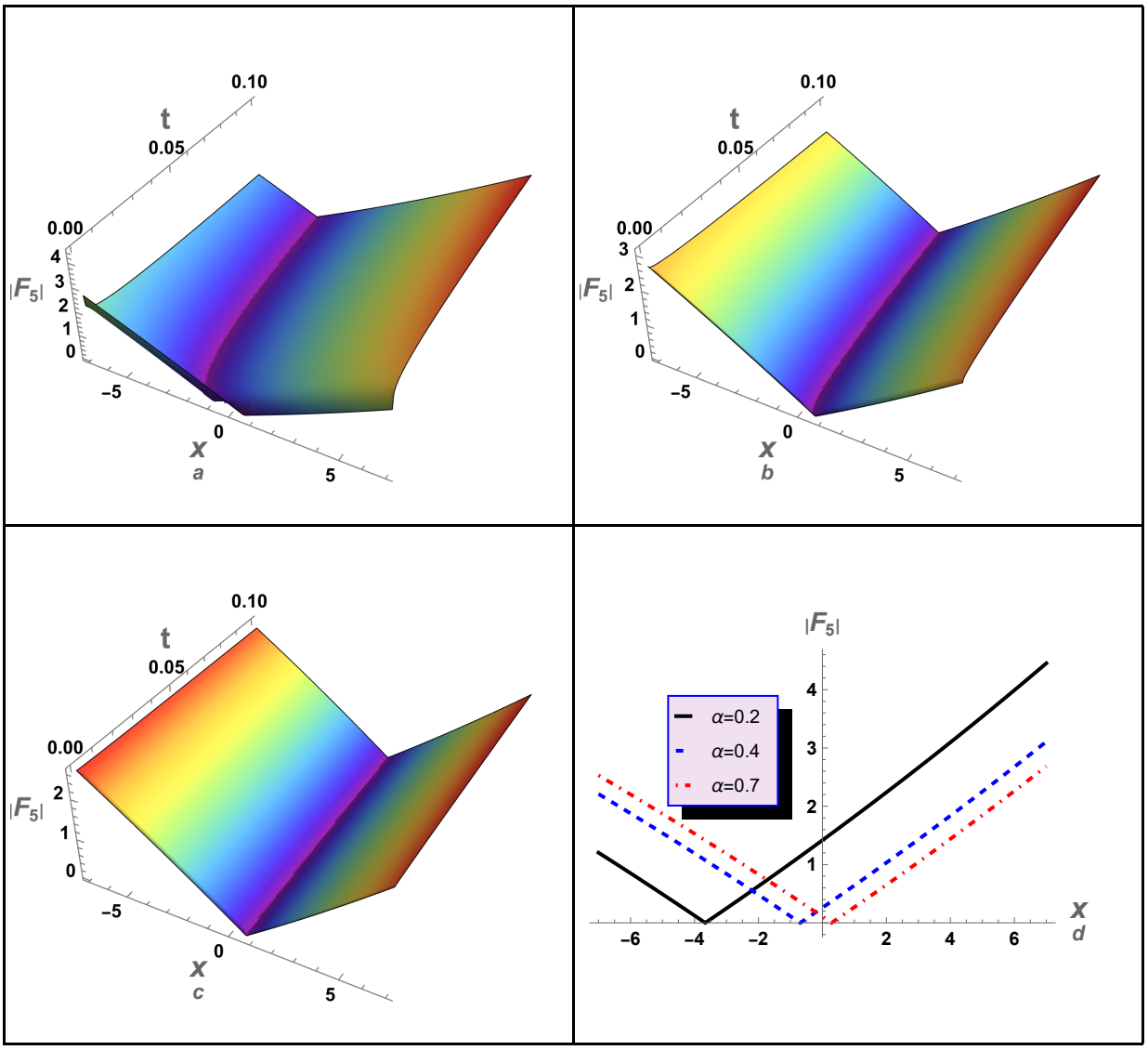

Figure 10. The solution $|F_5(x,t)|$ is plotted against the time-fractional parameter α: (a) 3D graphic for the solution given by Eq (3.11) at $\alpha = 0.2$, (b) 3D graphic for the solution given by Eq (3.11) at $\alpha = 0.4$, (c) 3D graphic for the solution given by Eq (3.11) at $\alpha = 0.7$, (d) 2D graphic for the solution given by Eq (3.11) at different values of α. Here, $\beta = 1$, $\lambda = -2$, $\mu = -2$, $\chi = 10$, $A = 0.1$, and $B = 10$.

5. Conclusion

The fractional DGH equation has been analytically solved by using the Riccati-Bernoulli sub-optimal differential equation method together with the Bäcklund transformation. We correctly obtained several travelling wave solutions in the form of hyperbolic, periodic, and rational solutions by applying the given norm; yielding a hierarchy of traveling wave solutions, including the quasi-peakon wave, shock-like wave, compacton-like wave, and other periodic waves. The resultant solutions were subjected to numerical analysis, wherein some random values were assigned to the

related coefficients and parameters. The effects of both space- and time-fractional parameters on the properties and behavior of all derived solutions was also examined. It has been found that the behavior of the derived solutions is significantly influenced by changing the values of both the space- and time-fractional parameters. By altering these parameters we found that, they not only affect the amplitude and width of the waves described by these solutions they also impact the transition between the waves. This finding represents a crucial outcome of our research. The obtained results demonstrate that the employed techniques are a direct and effective strategy for addressing highly complicated and strong nonlinear evolution/wave equations. They yield a substantial number of analytical solutions, which can help many researchers interpret their distinct results.

It is essential to acknowledge that the numerical analysis of the acquired results and the graphical representation of the derived solutions were conducted by using Wolfram MATHEMATICA 13.2.

Future work: The results indicate that the current technique offers many analytical solutions, allowing researchers to utilize this approach to simulate various physical and engineering problems. Thus, this approach is expected to efficiently examine and simulate a range of evolution/wave equations that describe various nonlinear phenomena in different plasma models. One example of its use is the analysis of the space-time fractional KdV-type equations [52, 53] and the space-time fractional Kawahara-type equations [54–56], which allows for an examination of the impact of fractional parameters on the generated solutions' profiles. Therefore, it is possible to study the effects of fractional coefficients on the behavior of the nonlinear structures described by these families of KdV-type and Kawahara-type equations, such as solitary waves, shock waves, cnoidal waves, and periodic waves. Furthermore, this method can be applied to examine nonlinear Schrödinger-type equations to investigate the impact of fractional parameters on the characteristics of envelope-modulated waves, such as bright and dark envelope solitons, rogue waves, and breathers, and modulated cnoidal waves [57, 58]. Therefore, this method is expected to have promising, effective, and fertile results in that can help to explain many mysterious nonlinear phenomena that arise and propagate in various plasma models.

Author contributions

Humaira Yasmin, Haifa A. Alyousef, Sadia Asad, Imran Khan, R. T. Matoog, S. A. El-Tantawy: writing, review, editing, and visualization. All authors of this article have been contributed equally. All authors have read and approved the final version of the manuscript for publication.

Use of AI tools declaration

The authors declare that they have not used Artificial Intelligence tools in the creation of this article.

Acknowledgments

The authors express their gratitude to Princess Nourah bint Abdulrahman University Researchers Supporting Project Number (PNURSP2024R17), Princess Nourah bint Abdulrahman University, Riyadh, Saudi Arabia. This work was supported by the Deanship of Scientific Research, Vice Presidency for Graduate Studies and Scientific Research, King Faisal University, Saudi Arabia (GrantA152).

Funding

The authors express their gratitude to Princess Nourah bint Abdulrahman University Researchers Supporting Project Number (PNURSP2024R17), Princess Nourah bint Abdulrahman University, Riyadh, Saudi Arabia. This work was supported by the Deanship of Scientific Research, Vice Presidency for Graduate Studies and Scientific Research, King Faisal University, Saudi Arabia (GrantA152).

Conflict of interest

The authors declare that they have no conflicts of interest.

References

1. M. A. Helal, A. R. Seadawy, M. H. Zekry, Stability analysis solutions for the sixth-order nonlinear Boussinesq water wave equations in two-dimensions, *Chin. J. Phys.*, **55** (2017), 378–385.
2. M. Arshad, A. R. Seadawy, D. Lu, J. Wang, Travelling wave solutions of Drinfel'd-sokolov-wilson, Whithambroer-kaup and (2+1)-dimensional Broer-Kaup-Kupershmit equations and their applications, *Chin. J. Phys.*, **55** (2017), 780–797.
3. D. Kumar, A. R. Seadawy, A. K. Joardar, Modified Kudryashov method via new analytic solutions for some conformable fractional differential equations arising in mathematical biology, *Chin. J. Phys.*, **56** (2018), 75–85.
4. M. K. Elboree, Lump solitons, rogue wave solutions and lump-stripe interaction phenomena to an extended (3+1)-dimensional KP equation, *Chin. J. Phys.*, **63** (2020), 290–303.
5. A. Riaz, R. Ellahi, M. M. Bhatti, M. Marin, Study of heat and mass transfer in the Eyring-Powell model of fluid propagating peristaltically through a rectangular compliant channel, *Heat Trans. Res.*, **50** (2019), 1539–1560.
6. M. M. Bhatti, R. Ellahi, A. Zeeshan, M. Marin, N. Ijaz, Numerical study of heat transfer and Hall current impact on peristaltic propulsion of particle-fluid suspension with compliant wall properties, *Modern Phys. Lett. B*, **33** (2019), 1950439.
7. H. Yasmin, N. H. Aljahdaly, A. M. Saeed, Investigating families of soliton solutions for the complex structured coupled fractional biswas-arshed model in birefringent fibers using a novel analytical technique, *Fractal Fract.*, **7** (2023), 491.
8. T. Botmart, R.P. Agarwal, M. Naeem, A. Khan, On the solution of fractional modified Boussinesq and approximate long wave equations with non-singular kernel operators, *AIMS Mathematics*, **7** (2022), 12483–12513. https://doi.org/10.3934/math.2022693
9. H. Yasmin, N. H. Aljahdaly, A. M. Saeed, Probing families of optical soliton solutions in fractional perturbed Radhakrishnan-Kundu-Lakshmanan model with improved versions of extended direct algebraic method, *Fractal Fract.*, **7** (2023), 512.
10. R. Shah, H. Khan, D. Baleanu, Fractional Whitham-Broer-Kaup equations within modified analytical approaches, *Axioms*, **8** (2019), 125.
11. P. Sunthrayuth, A. M. Zidan, S. W. Yao, M. Inc, The comparative study for solving fractional-order Fornberg-Whitham equation via ρ-Laplace transform, *Symmetry*, **13** (2021), 784.

12. X. Gao, Two-layer-liquid and lattice considerations through a (3+1)-dimensional generalized Yu-Toda-Sasa-Fukuyama system, *Appl. Math. Lett.*, **152** (2024), 109018.
13. X. Gao, Considering the wave processes in oceanography, acoustics and hydrodynamics by means of an extended coupled (2+1)-dimensional Burgers system, *Chin. J. Phys.*, **86** (2023), 572–577.
14. X. Gao, Oceanic shallow-water investigations on a generalized Whitham–Broer–Kaup–Boussinesq–Kupershmidt system, *Phys. Fluids*, **35** (2023), 127106. https://doi.org/10.1063/5.0170506
15. Y. Shen, B. Tian, T. Zhou, C. Cheng, Multi-pole solitons in an inhomogeneous multi-component nonlinear optical medium, *Chaos, Soliton. Fract.*, **171** (2023), 113497.
16. T. Y. Zhou, B. Tian, Y. Shen, Auto-Bäcklund transformations and soliton solutions on the nonzero background for a (3+1)-dimensional Korteweg-de Vries-Calogero-Bogoyavlenskii-Schif equation in a fluid, *Nonlinear Dyn.* **111** (2023), 8647–8658.
17. S. Meng, F. Meng, F. Zhang, Q. Li, Y. Zhang, A. Zemouche, Observer design method for nonlinear generalized systems with nonlinear algebraic constraints with applications, *Automatica*, **162** (2024), 111512. https://doi.org/10.1016/j.automatica.2024.111512
18. Y. Shi, C. Song, Y. Chen, H. Rao, T. Yang, Complex Standard Eigenvalue Problem Derivative Computation for Laminar-Turbulent Transition Prediction, *AIAA J.*, **61** (2023), 3404–3418. https://doi.org/10.2514/1.J062212
19. X. Cai, R. Tang, H. Zhou, Q. Li, S. Ma, D. Wang, L. Zhou, Dynamically controlling terahertz wavefronts with cascaded metasurfaces, *Adv. Photonics*, **3** (2021), 036003. https://doi.org/10.1117/1.AP.3.3.036003
20. A. Saad Alshehry, M. Imran, A. Khan, W. Weera, Fractional view analysis of Kuramoto-Sivashinsky equations with non-singular kernel operators, *Symmetry*, **14** (2022) 1463.
21. H. M. Srivastava, H. Khan, M. Arif, Some analytical and numerical investigation of a family of fractional-order Helmholtz equations in two space dimensions, *Math. Methods Appl. Sci.*, **43** (2020), 199–212.
22. H. Yasmin, N. H. Aljahdaly, A. M. Saeed, R. Shah, Investigating symmetric soliton solutions for the fractional coupled konno-onno system using improved versions of a novel analytical technique, *Mathematics*, **11** (2023), 2686.
23. M. M. Al-Sawalha, A. Khan, O. Y. Ababneh, T. Botmart, Fractional view analysis of Kersten-Krasil'shchik coupled KdV-mKdV systems with non-singular kernel derivatives, *AIMS Mathematics*, **7** (2022), 18334–18359. http://doi.org/10.3934/math.20221010
24. A. A. Alderremy, N. Iqbal, S. Aly, K. Nonlaopon, Fractional series solution construction for nonlinear fractional reaction-diffusion Brusselator model utilizing Laplace residual power series, *Symmetry*, **14** (2022), 1944.
25. T. A. A. Ali, Z. Xiao, H. Jiang, B. Li, A Class of Digital Integrators Based on Trigonometric Quadrature Rules, *IEEE Trans. Ind. Electron.*, **71** (2024), 6128–6138. https://doi.org/10.1109/TIE.2023.3290247
26. C. Guo, J. Hu, Time base generator based practical predefined-time stabilization of high-order systems with unknown disturbance, *IEEE T. Circuits II*, **70** (2023), 2670–2674. https://doi.org/10.1109/TCSII.2023.3242856

27. Y. Kai, Z. Yin, Linear structure and soliton molecules of Sharma-Tasso-Olver-Burgers equation, *Phys. Lett. A*, **452** (2022), 128430. doilinkhttps://doi.org/10.1016/j.physleta.2022.128430
28. S. S. Ray, R. K. Bera, Analytical solution of a fractional diffusion equation by Adomian decomposition method, *Appl. Math. Comput.*, **174** (2006), 329–336.
29. B. K. Singh, P. Kumar, Fractional variational iteration method for solving fractionalpartial differential equations with proportional delay, *Int. J. Differ. Equ.*, **2017** (2017), 11. https://doi.org/10.1155/2017/5206380
30. J. Chen, F. Liu, V. Anh, Analytical solution for the time-fractional telegraph equation by the method of separating variables, *J. Math. Anal. Appl.*, **338** (2008), 1364–1377.
31. Y. Nikolova, L. Boyadjiev, Integral transforms method to solve a time-space fractional diffusion equation, *Fract. Calculus Appl. Anal.*, **13** (2010), 57–68.
32. M. S. Rawashdeh, H. Al-Jammal, New approximate solutions to fractional nonlinear systems of partial differential equations using the FNDM, *Adv. Differ. Equ.*, **2016** (2016), 235. https://doi.org/10.1186/s13662-016-0960-x
33. A. Elsaid, S. Shamseldeen, S. Madkour, Analytical approximate solution of fractional wave equation by the optimal homotopy analysis method, *Eur. J. Pure Appl. Math.*, **10** (2017), 586–601.
34. R. K. Saxena, S. L. Kalla, On the solutions of certain fractional kinetic equations, *Appl. Math. Comput.*, **199** (2008), 504–511.
35. A, Cetinkaya, O. Kymaz, The solution of the time-fractional diffusion equation by the generalized differential transform method, *Math. Comput. Modell.*, **57** (2013), 2349–2354.
36. H, Khan, S, Barak, P, Kumam, M. Arif, Analytical Solutions of Fractional Klein-Gordon and Gas Dynamics Equations, via the G/G'-Expansion Method, *Symmetry*, **11** (2019), 566.
37. Y,Kai, J, Ji, Z. Yin, Study of the generalization of regularized long-wave equation, *Nonlinear Dynamics*, **107** (2022), 2745–2752. https://doi.org/10.1007/s11071-021-07115-6
38. Q, Han, F. Chu, Nonlinear dynamic model for skidding behavior of angular contact ball bearings, *J. Sound Vib.*, **354** (2015), 219–235. https://doi.org/10.1016/j.jsv.2015.06.008
39. M. A. E. Abdelrahman, M. A. Sohaly, Solitary waves for the modified Korteweg-de Vries equation in deterministic case and random case, *J. Phys. Math.*, **8** (2017), 214. https://doi.org/10.4172/2090-0902.1000214
40. M. A. E. Abdelrahman, M. A. Sohaly, Solitary waves for the nonlinear Schrödinger problem with the probability distribution function in the stochastic input case, *Eur. Phys. J. Plus.*, **132** (2017), 339.
41. X. F. Yang, Z. C. Deng, Y. Wei, A Riccati-Bernoulli sub-ODE method for nonlinear partial differential equations and its application, *Adv. Diff. Equa.*, **1** (2015), 117–133.
42. H. R. Dullin, G. A. Gottwald, D. D. Holm, An integrable shallow water equation with linear and nonlinear dispersion, *Phys. Rev. Lett.*, **87** (2001), 194501.
43. H. R. Dullin, G. A. Gottwald, D. D. Holm, On asymptotically equivalent shallow water wave equations, *Physica. D.*, **190** (2004), 1–14.
44. L. X. Tian, G. Gui, Y. Liu, On the well-posedness problem and the scattering problem for the Dullin–Gottwald–Holm Equation, *Commun. Math. Phys.*, **257** (2005), 667–701.

45. M. Y. Tang, C. X. Yang, Extension on peaked wave solutions of CH-γ equation, *Chaos Soliton. Fract.*, **20** (2004), 815–825.
46. C. L. Chen, Y. S. Li, J. E. Zhang, The multi-soliton solutions of the CH-γ equation, *Sci. China Ser. A-Math.*, **51** (2008), 314–320. https://doi.org/10.1007/s11425-007-0137-x
47. L. J. Zhang, L. Q. Chen, X. W. Huo, Peakons and periodic cusp wave solutions in a generalized Camassa–Holm equation, *Chaos Soliton. Fract.*, **30** (2006), 1238–1249.
48. Y. Liu, Global existence and blow-up solutions for a nonlinear shallow water equation, *Math. Ann.*, **335** (2006), 717–735.
49. H. R. Dullin, G. A. Gottwald, D. D. Holm, Camassa–Holm, Korteweg–de Vries-5 and other asymptotically equivalent equations for shallow water waves, *Fluid Dyn. Res.*, **33** (2003), 73–95.
50. M. Z. Sarikaya, H. Budak, H. Usta, On generalized the conformable fractional calculus, *TWMS J. Appl. Eng. Math.*, **9** (2019), 792799.
51. D. Lu, Q. Shi, New Jacobi elliptic functions solutions for the combined KdV-mKdV equation, *Int. J. Nonlinear Sci.*, **10** (2010), 320–325.
52. S. A. Almutlak, S. Parveen, S. Mahmood, A. Qamar, B. M. Alotaibi, S. A. El-Tantawy, On the propagation of cnoidal wave and overtaking collision of slow shear Alfvén solitons in low $\beta-$magnetized plasmas, *Phys. Fluids*, **35** (2023), 075130. https://doi.org/10.1063/5.0158292
53. T. Hashmi, R. Jahangir, W. Masood, B. M. Alotaibi, S. M. E, Ismaeel, S. A. El-Tantawy, Head-on collision of ion-acoustic (modified) Korteweg-de Vries solitons in Saturn's magnetosphere plasmas with two temperature superthermal electrons, *Phys. Fluids*, **35** (2023), 103104.
54. R. A. Alharbey, W. R. Alrefae, H. Malaikah, E. Tag-Eldin, S. A. El-Tantawy, Novel approximate analytical solutions to the nonplanar modified Kawahara equation and modeling nonlinear structures in electronegative plasmas, *Symmetry*, **15** (2023), 97.
55. S. A. El-Tantawy, A. H. Salas, H. A. Alyouse, M. R. Alharthi, Novel exact and approximate solutions to the family of the forced damped Kawahara equation and modeling strong nonlinear waves in a plasma, *Chin. J. Phys.*, **77** (2022), 2454.
56. M. R. Alharthi, R. A. Alharbey, S. A. El-Tantawy, Novel analytical approximations to the nonplanar Kawahara equation and its plasma applications, *Eur. Phys. J. Plus*, **137** (2022), 1172.
57. M. Irshad, Ata-ur-Rahman, M. Khalid, S. Khan, B. M. Alotaibi, L. S. El-Sherif, S. A. El-Tantawy, Effect of κ-deformed Kaniadakis distribution on the modulational instability of electron-acoustic waves in a non-Maxwellian plasma, *Phys. Fluids*, **35** (2023), 105116. https://doi.org/10.1063/5.0171327
58. S. A. El-Tantawy, T. Aboelenen, Simulation study of planar and nonplanar super rogue waves in an electronegative plasma: Local discontinuous Galerkin method, *Phys. Plasmas*, **24** (2017), 052118. https://doi.org/10.1063/1.4983327

AIMS Press